coatings

MDPI

Article

Effect of Surface Pretreatment on Quality and Electrochemical Corrosion Properties of Manganese Phosphate on S355J2 HSLA Steel

Filip Pastorek [1,*], Kamil Borko [2], Stanislava Fintová [3,4], Daniel Kajánek [1,2] and Branislav Hadzima [1,2]

1 Research Centre, University of Zilina, Zilina 010 08, Slovakia; daniel.kajanek@fstroj.uniza.sk (D.K.); branislav.hadzima@rc.uniza.sk (B.H.)
2 Department of Materials Engineering, Faculty of Mechanical Engineering, University of Zilina, Zilina 010 08, Slovakia; kamil.borko@fstroj.uniza.sk
3 Institute of Physics of Materials, Academy of Science of the Czech Republic, Brno 616 62, Czech Republic; fintova@ipm.cz
4 CEITEC IPM, Institute of Physics of Materials, Academy of Sciences of the Czech Republic, Brno 616 62, Czech Republic
* Correspondence: filip.pastorek@rc.uniza.sk; Tel.: +421-41-513-7622

Academic Editor: Robert B. Heimann
Received: 5 September 2016; Accepted: 11 October 2016; Published: 15 October 2016

Abstract: High strength low alloy (HSLA) steels exhibit many outstanding properties for industrial applications but suffer from unsatisfactory corrosion resistance in the presence of aggressive chlorides. Phosphate coatings are widely used on the surface of steels to improve their corrosion properties. This paper evaluates the effect of a manganese phosphate coating prepared after various mechanical surface treatments on the electrochemical corrosion characteristics of S355J2 steel in 0.1 M NaCl electrolyte simulating aggressive sea atmosphere. The manganese phosphate coating was created in a solution containing H_3PO_4, MnO_2, dissolved low carbon steel wool, and demineralised H_2O. Scanning electron microscopy (SEM) was used for surface morphology observation supported by energy-dispersive X-ray analysis (EDX). The electrochemical corrosion characteristics were assessed by electrochemical impedance spectroscopy (EIS) and potentiodynamic polarization (PD) measurements in the solution of 0.1 M NaCl. Method of equivalent circuits and Tafel-extrapolation were used for the analysis of the obtained results. Performed experiments and analysis showed that the morphological and corrosion properties of the surface with manganese phosphate are negatively influenced by sandblasting surface pretreatment.

Keywords: corrosion; steel; sandblasting; manganese phosphate

1. Introduction

The prime motivation of developing high strength low alloy (HSLA) steels was the replacement of low-carbon steels for the automotive industry in order to improve their strength-to-weight ratio and meet the need for higher-strength construction grade materials. HSLA steels have excellent strength, good weldability and ductility, and also outstanding low temperature impact toughness superior to that of high yield strength (HY) steels [1]. However, proper surface treatment is necessary for many applications to increase their resistance to aggressive environment.

One of the most commonly used method for surface preparation is sandblasting, used for various purposes of surface influence including: modification [2], strengthening [3], cleaning and rust removal [4]. Sandblasting abrasive particles are smaller compared with particles in shot peening technology and lower pressure of compressed air is used. Therefore, a smoother surface can be

obtained by sandblasting in general. During the sandblasting process, the surface of samples is blasted repeatedly by sand particles or other hard particles with high speed, which leads to the removal of oxide scale and generation of local plastic deformation in the surface layer. However, Wang et al. [5] observed decrease of corrosion resistance of steel after sandblasting resulting from the existence of high-density lattice defect: dislocation, that limits the application possibilities of this technique [6,7].

Phosphate coatings are the preferred surface treatment of several alloys since they exhibit a good adhesion, good corrosion resistance, improved abrasive resistance of the structures and a low cost in comparison with other coating systems [8]. The main types of phosphate coatings are manganese, iron, and zinc based [9,10].

Manganese phosphate coatings exhibit outstanding lubricant retention properties and mechanical resistance. Excellent corrosion resistance and anti-galling properties are the results of uniform crystal size distributions and high coating weight [11]. As revealed by accelerated corrosion tests, manganese phosphate demonstrates the best corrosion resistance compared to zinc and iron phosphates [12]. Manganese phosphate coating can be used on high strength steels for the oil and gas extraction industry [11]. Sufficient quality of phosphate coatings is reached by proper control of process and material parameters including: composition of the metal, structure of the metal surface, surface preparation, pH, bath chemical composition, time, temperature, etc. [8,13] There are many studies focused on corrosion properties of various phosphate coatings on various steels [8,10–12,14,15] but no deeper research is performed on how sandblasting influences the electrochemical properties of manganese phosphate on HSLA steels. For these reasons, the aim of this study is to investigate this phenomenon.

2. Materials and Methods

S355J2 steel was used for the experimental investigation. The chemical composition of this steel can be found in Table 1. The microstructure was observed by the light metallographic microscope CARL ZEISS AXIO Imager.A1m (ZEISS, Oberkochen, Germany), equipment financed by the project ITMS 26220220121). All the samples were prepared by standard metallographic methods. 3% Nital was used as an etchant for visualization of the S355J2 steel microstructure.

Table 1. Composition of S355J2 steel.

Component	C	Mn	P	S	Si	Cu	Fe
wt %	0.200	1.600	0.025	0.025	0.550	0.550	balance

S355J2 steel samples were ground (p500 grit SiC paper) to reach the homogenous surface roughness. Some samples were further sandblasted. Sandblasting was performed by sand particles on a mobile pressure sandblasting machine with a nozzle diameter 6 mm and pressure of 0.6 MPa. The final operation was chemical treatment of both surfaces by manganese phosphating (MnP). Composition of phosphating bath was 300 mL of demineralised water, 4.49 g of H_3PO_4, the same amount of MnO_2 and 3 g of ultrafine low carbon steel wool of the grade 0000 (mean width of fibres 15.24–25.4 μm). After the initial dissolving of the steel wool in phosphate solution at 90 to 95 °C the subsequent phosphating of the samples was performed for 75 min at the same temperature of 90 to 95 °C. Demineralised water and ethanol were used for cleaning of the samples after final surface treatment, followed by dried air streaming to remove chemical and mechanical residues.

The phosphating mechanism was initially described by Ghali and Potvin [16]. The phosphating process consists of four stages: (1) initial substrate dissolution caused by medium acidity. This dissolution leads to an increase of the bath pH value by the hydrogen evolution reaction (HER); (2) massive precipitation of very fine phosphate particles; (3) phosphate crystallization and growth; and (4) reorganization of the crystals, i.e., high rate dissolution and re-precipitation of the phosphate in the coating that reduce the exposed area and coating porosity. This mechanism was originally

observed in the zinc phosphating process, but can be theoretically adopted for manganese phosphating also [11,16]. Dissolution of ultrafine low carbon steel wool helps to add Fe^{2+} ions to the phosphate solution, reduces the first stage of phosphating causing the dissolution of substrate surface and supports the second phosphating stage.

The manganese phosphate morphology was observed by scanning electron microscopy (SEM) LYRA3 TESCAN and chemical analysis of coatings was realized by energy dispersive X-ray (EDX) technique. Cross section images were taken by light metallographic microscopy (LM). Surface roughness was measured by surface roughness tester Mitutoyo SJ-210 according to ISO 4287–1997 standard focusing on maximum roughness (R_z) and arithmetic average (R_a) values [17]. Thermodynamic corrosion electrochemical characteristics (corrosion potential) together with kinetic corrosion electrochemical characteristics (corrosion current density and corrosion rate) and electrochemical impedance spectroscopy corrosion characteristics (polarization resistance) were assessed by corrosion tests in a solution simulating aggressive sea environment (0.1 M NaCl) at ambient temperature. A cell composed of three electrodes (counter electrode, working electrode and reference electrode) was used for electrochemical tests. The potentiodynamic polarization (PD) measurements and electrochemical impedance spectroscopy (EIS) measurements were realized by potentiostat VSP from BioLogic SAS France (equipment financed by the project ITMS 26220220048). EIS measurements were running under potential control with scanning frequency range 100 kHz–10 mHz [18]. The perturbation amplitude was 10 mV and stabilization time in NaCl solution was set to 5 min.

The PD curves were obtained at ambient temperature using an applied potential from −250 mV to +250 mV vs. open circuit potential with a constant voltage step 1 $mV \cdot s^{-1}$ as used by Taghavikish et al. [19]. Measured potentiodynamic curves were analyzed using Tafel fit by EC-Lab software (software financed by the project ITMS 26220220183). The obtained diagrams were expressed in semi-logarithmic scale in order to reach better interpretation of the measured data. The PD measurements were performed at least three times, so that reproducibility of the test results was ensured [20].

3. Results and Discussion

Figure 1 shows the microstructure of tested S355J2 steel. The microstructure revealed ferrite-pearlite matrix with a low pearlite content (local pearlite occurrence) and with average grain size of 10 μm.

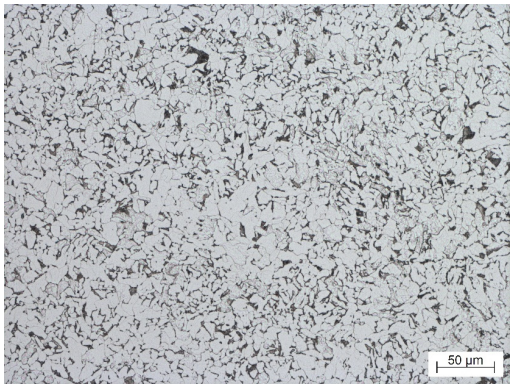

Figure 1. Microstructure of etched S355J2 steel.

The coatings produced on steel from manganese phosphate solutions consist almost entirely of hurealite $(Mn,Fe)_5H_2(PO_4)_4 \cdot 4H_2O$. They may also contain variable amounts of secondary and tertiary ferrous phosphates. Iron and manganese in hurealite are mutually replaceable [21]. The evidence of proper hurealite formation on the surface of S355J2 steel was confirmed by performed EDX analysis

(Figure 2). The major form of hurealite was $Mn_5H_2(PO_4)_4 \cdot 4H_2O$ as obvious from the almost doubled concentration of Mn in the phosphate surface layer compared to Fe.

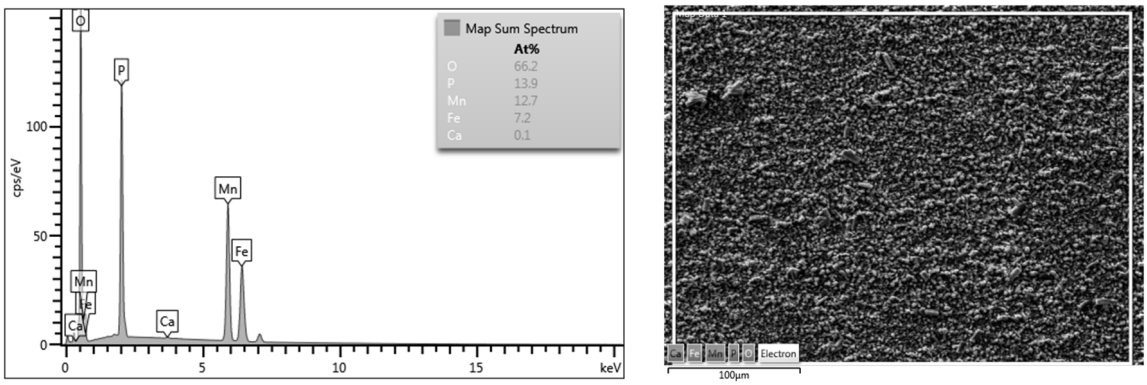

Figure 2. EDX analysis of created phosphate layer.

The surface morphologies of phosphate coating formed on ground and sandblasted surfaces are shown in Figure 3 and their cross section images are shown in Figure 4. Moderate grinding of the steel surface prior to phosphating leads to the formation of thin (4 to 9 µm) but very continuous and homogenous phosphate coating with a crystal size from 1 to 5 µm. Crystal organization is very compact and reveals a minimum of defect areas. On the other hand, the phosphate coating formed on a sandblasted surface is thicker on average (thickness ranges from 3 up to 12 µm) compared to a ground surface but there is an obvious inhomogeneity and frequent occurrence of coating defects and pores of different size. Crystals are of irregular shape, more elongated compared to crystals formed on a ground surface with a size ranging from 1 to 7 µm. Sandblasted surface has significantly higher roughness as seen from Table 2. Moreover, sandblasting causes more intensive surface deformation that is responsible for the increase of dislocations and defect numbers, and for higher thermodynamic differences between local surface micro areas in comparison to ground surface. This inhomogeneity is then reflected in non-uniform coating formation. Crystal nucleation and further growth is preferentially present in the micro areas with increased inner energy (small residual stresses after sandblasting).

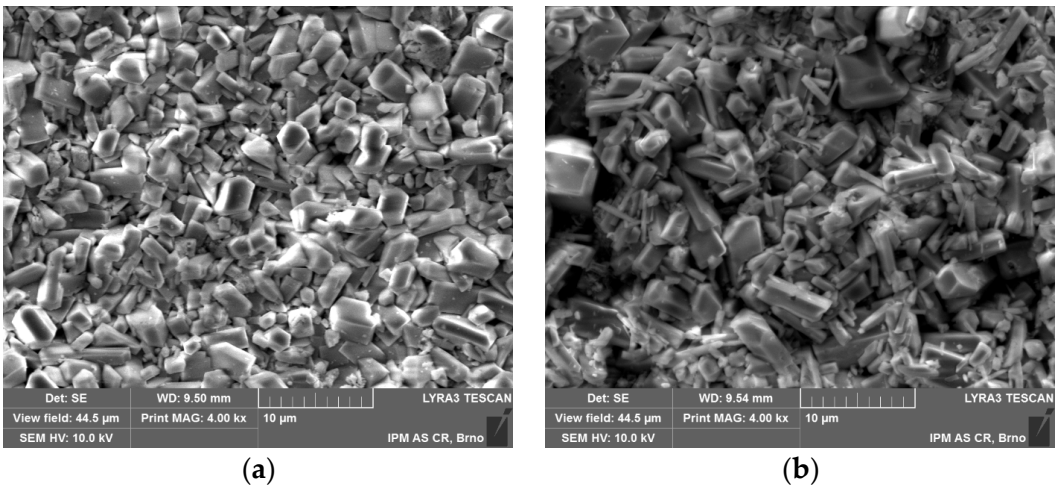

(**a**) (**b**)

Figure 3. SEM images of phosphate surface morphology on: (**a**) ground surface; (**b**) sandblasted surface.

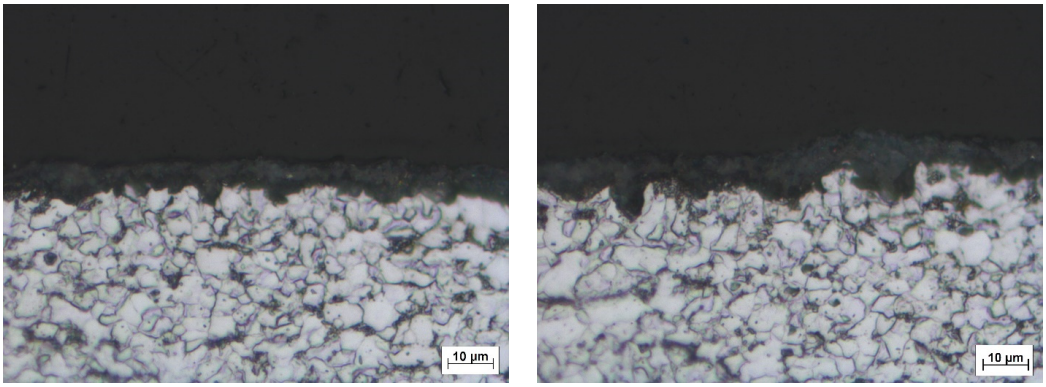

(**a**) (**b**)

Figure 4. Cross-section images of MnP phosphate surface on: (**a**) ground surface; (**b**) sandblasted surface.

Table 2. Measured surface roughness parameters of the samples with different surface treatment.

Surface Treatment Roughness Parameters	Ground (p500)	Sandblasted	Ground + MnP	Sandblasted + MnP
R_a (µm)	0.28	1.67	0.67	1.29
R_z (µm)	1.99	12.70	5.15	9.40

Figure 5 shows the measured potentiodynamic curves of S355J2 steel samples after various surface treatments in 0.1 M NaCl corrosive solution. Measured kinetic and thermodynamic corrosion characteristics together with Tafel constants (β_a and β_c) values are listed in Table 3. Mechanical and chemical surface treatments caused changes in both thermodynamic and kinetic characteristics of the base material. Thermodynamic stability of the surface is represented by the values of corrosion potentials E_{corr} in our case. More positive value of this electrochemical characteristic means that the surface is nobler and thermodynamically more stable. The kinetics of the corrosion process are expressed by the corrosion current density i_{corr} reflecting the intensity of running corrosion processes in an electrolyte. This electrochemical characteristic has a direct relation to the corrosion rate r_{corr} [22]. Sandblasting caused a more intensive attack of the steel surface compared to grinding. A destroyed surface with a higher concentration of structure defects and with larger area of an active surface resulted in lower electrochemical stability, which is reflected in the 51 mV decrease of E_{corr} value in comparison with a simply ground surface. A part of the kinetic energy of the sandblasting particles transformed to added internal energy of the base material, which caused its absolute value to increase. As the result of higher surface activity, an increase is observed of the corrosion current density i_{corr} and the directly related value of corrosion rate r_{corr} on sandblasted surface compared to the ground surface. However, this increase is not very significant and represents just 1.3 $\mu A \cdot cm^{-2}$ (29 $\mu m \cdot y^{-1}$). It is a beneficial finding that the corrosion resistance decrease caused by intensive sandblasting during surface cleaning is acceptable. The fact that sandblasting deteriorates corrosion properties was observed on stainless steel [7] as well as pure titanium [23]. Manganese phosphating significantly improved both thermodynamic and kinetic characteristics of the steel surface after both mechanical pretreatment operations (grinding and sandblasting). However, the negative influence of sandblasting on surface corrosion properties persisted. By forming a stable layer several microns thick, manganese phosphate forms a mechanical barrier against corrosion. The higher stability of manganese phosphate in 0.1 M NaCl solution compared to the base metal resulted in considerably more positive values of E_{corr}. The positive shift was 252 mV on ground surface and 250 mV on sandblasted surface, a negligible difference. The most positive and noble value of E_{corr} was reached with ground and subsequently phosphated surface (−399 mV). Thanks to the mechanical barrier action of manganese phosphate,

the diffusion of oxygen to base metal active surface is more difficult and concentrated mainly in more porous areas. This complication of the kinetics of the corrosion process results in a decrease of i_{corr} and r_{corr} values of both phosphated surfaces. Creation of uniform phosphate surface coating on ground surface led to almost 17-fold reduction of the corrosion rate and almost 13-fold reduction on sandblasted surface. The lowest kinetic corrosion characteristics were again reached with ground and subsequently phosphated surface. Phosphate treatment chiefly influences the anodic reaction as seen from almost double values of β_a reached after phosphating.

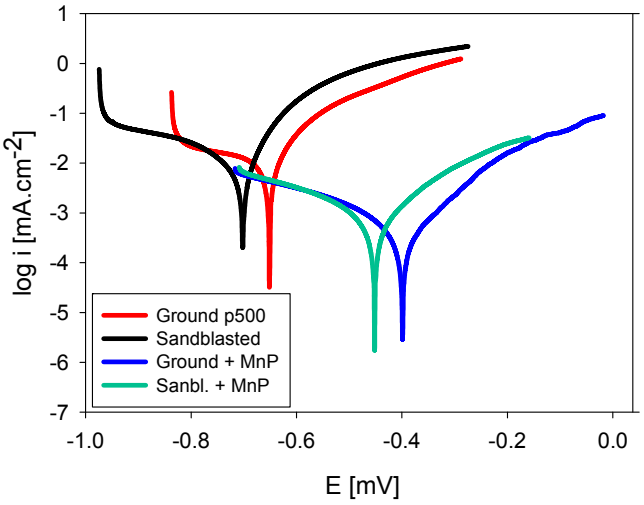

Figure 5. Potentiodynamic curves of S355J2 steel after various surface treatments in 0.1 M NaCl.

Table 3. Measured electrochemical corrosion characteristics.

Electrochemical Characteristics Surface Treatment	E_{corr} (mV_{SCE})	i_{corr} ($\mu A \cdot cm^{-2}$)	r_{corr} ($\mu m \cdot y^{-1}$)	β_a ($mV \cdot dec^{-1}$)	β_c ($mV \cdot dec^{-1}$)
Ground (p500)	-651 ± 10	8.7 ± 0.2	202 ± 4	84 ± 5	350 ± 7
Sandblasted	-702 ± 15	10.0 ± 0.2	231 ± 5	82 ± 6	283 ± 7
Ground + MnP phosphated	-399 ± 22	0.5 ± 0.1	12 ± 1	152 ± 11	268 ± 12
Sandblasted + MnP phosphated	-452 ± 25	0.8 ± 0.1	18 ± 1	159 ± 13	250 ± 10

The findings from potentiodynamic polarization tests were supported by non-destructive electrochemical impedance spectroscopy (EIS) measurements. Figure 6 shows the Nyquist diagrams of S355J2 steel samples after various surface treatment. Nyquist plots are frequently selected tool for EIS interpretation, allowing precise determination of equivalent circuit components [22,24,25]. Figure 7 shows the equivalent circuit best describing the electrochemical processes at the sample-electrolyte interface. Polarization resistance R_p is the most important electrochemical characteristic. The value of R_p expresses how resistant the mono- or multi- surface layers are against corrosion [26–28]. Component CPE represents a constant phase element. Its function in the expression of EIS data is defined elsewhere [25,29]. The values of equivalent circuit elements were obtained from the analysis of a selected equivalent circuit using a software EC-Lab (Bio-Logic Science Instruments SAS, Claix, France, version 11.01). These values are listed in Table 4. The highest value of R_p was reached with ground and subsequently phosphated surfaces. This value was 34 times higher compared to only ground surface and almost twice as high as on sandblasted and further phosphated surface, which is evidence of uniform manganese phosphate coating formation.

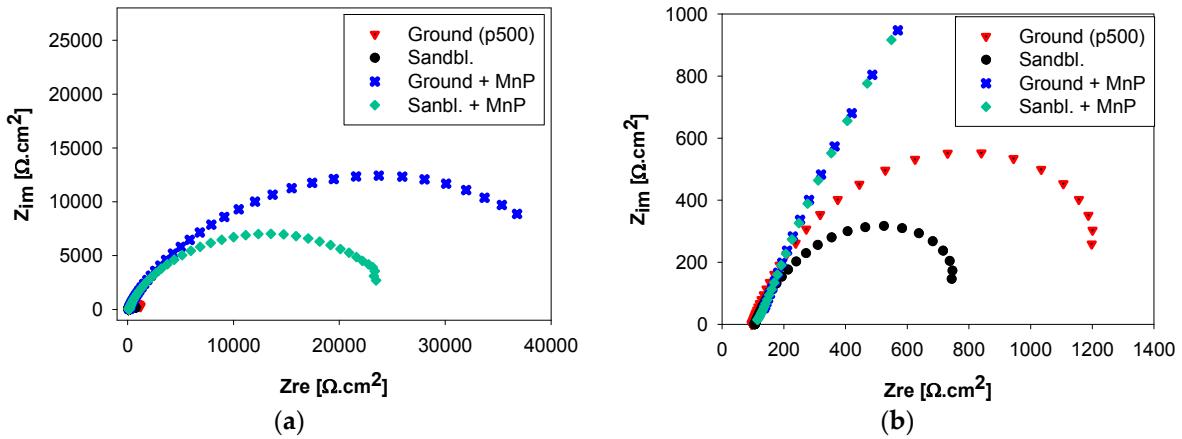

Figure 6. Measured Nyquist diagrams of S355J2 steel samples with different surface treatment (0.1 M NaCl solution): (**a**) overall view; (**b**) detail.

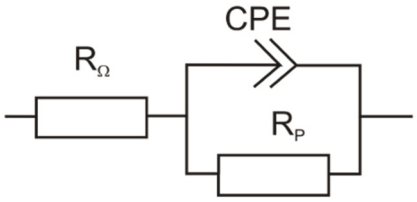

Figure 7. Equivalent circuit for Nyquist plots analyses.

Table 4. Electrochemical characteristics of S355J2 steel after various surface treatments.

Electrochemical Characteristics Surface Treatment	R_Ω ($\Omega \cdot cm^2$)	R_p ($\Omega \cdot cm^2$)	CPE ($10^{-6} \cdot F \cdot s^{n-1}$)	n
Ground (p500)	97 ± 3	1220 ± 53	538 ± 24	0.81 ± 0.02
Sandblasted	98 ± 4	770 ± 42	953 ± 33	0.79 ± 0.01
Ground + MnP phosphated	94 ± 4	41880 ± 627	1652 ± 34	0.69 ± 0.02
Sandblasted + MnP phosphated	95 ± 4	23600 ± 491	1924 ± 46	0.71 ± 0.03

Combination of complex surface morphology observations with complete electrochemical corrosion evaluation of tested surface treatments led to integrated findings. The sandblasting pretreatment generally helps to remove surface contaminants and corrosion products from the surface and forms rougher surfaces suitable for further painting operations. On the one hand, the quality and morphology of the sandblasted surface are responsible for rougher, less uniform, and more porous manganese phosphate coating in a comparison with manganese phosphate created on ground surfaces. On the other hand, increased surface roughness and porosity of the manganese coating are beneficial if additional painting or coating is applied in the case of improving integrity of whole coating system with the base metal. When the manganese phosphating represents the final surface treatment operation whereby higher quality and maximal corrosion protection are required, a more appropriate pretreatment process is a simple grinding.

4. Conclusions

The present work describes the influence of various surface treatments on morphological and corrosion properties of manganese phosphate on S355J2 steel. The most relevant conclusion is as follows:

- Using the manganese phosphating process created a continuous coating on the steel surface after both mechanical surface pretreatment techniques. However, the higher uniformity of the coating and crystal size together with lower porosity and defect occurrence was obtained on ground surfaces;
- Sandblasting caused increased surface roughness of the substrate compared to a ground surface. This influence was reduced after subsequent manganese phosphate formation;
- Sandblasting had a negative effect on the corrosion resistance of S355J2 steel compared to ground surfaces. Worsening was observed of the relevant electrochemical corrosion characteristics including E_{corr}, i_{corr}, r_{corr}, and R_p after sandblasting;
- The phosphate treatment reduces the corrosion rate as ascertained both in polarization curves and impedance tests by about the same extent on ground and sandblasted samples;
- Manganese phosphating results in an increase of the polarization resistance of the steel surface by more than 30 times.

Acknowledgments: The research has been supported by Science Grant Agency of the Slovak Republic through project No. 1/0720/14. Authors are grateful works to the Slovak Research and Development Agency for support in experimentalby the projects No. APVV-14-0284, No. APVV-14-0772 and No. APVV-14-0096. This research was carried out under the project CEITEC 2020 (LQ1601) with financial support from the Ministry of Education, Youth and Sports of the Czech Republic under the National Sustainability Programme II.

Author Contributions: Branislav Hadzima and Stanislava Fintová conceived and designed the experiments; Kamil Borko performed the experiments; Daniel Kajánek analysed the data; Filip Pastorek contributed reagents/materials/analysis tools; Filip Pastorek wrote the paper.

Conflicts of Interest: The authors declare no conflict of interest.

References

1. Nathan, S.R.; Balasubramanian, V.; Malarvizhi, S.; Rao, A.G. Effect of welding processes on mechanical and microstructural characteristics of high strength low alloy naval grade steel joints. *Def. Technol.* **2015**, *11*, 308–317. [CrossRef]
2. Chintapalli, R.K.; Marro, F.G.; Jimenez-Pique, E.; Anglada, M. Phase transformation and subsurface damage in 3Y-TZP after sandblasting. *Dent. Mater.* **2013**, *29*, 566–572. [CrossRef] [PubMed]
3. Chintapalli, R.K.; Mestra Rodriguez, A.; Garcia Marro, F.; Anglada, M. Effect of sandblasting and residual stress on strength of zirconia for restorative dentistry applications. *J. Mech. Behav. Biomed.* **2014**, *29*, 126–137. [CrossRef] [PubMed]
4. Raykowski, A.; Hader, M.; Maragno, B.; Spelt, J.K. Blast cleaning of gas turbine components: Deposit removal and substrate deformation. *Wear* **2001**, *249*, 126–131. [CrossRef]
5. Wang, X.Y.; Li, D.Y. Mechanical and electrochemical behavior of nanocrystalline surface of 304 stainless steel. *Electrochim. Acta* **2002**, *47*, 3939–3947. [CrossRef]
6. Trško, L.; Bokůvka, O.; Nový, F.; Guagliano, M. Effect of severe shot peening on ultra-high-cycle fatigue of a low-alloy steel. *Mater. Des.* **2014**, *57*, 103–113. [CrossRef]
7. Geng, S.; Sun, J.; Guo, L. Effect of sandblasting and subsequent acid pickling and passivation on the microstructure and corrosion behavior of 316L stainless steel. *Mater. Design.* **2015**, *88*, 1–7. [CrossRef]
8. Galvan-Reyes, C.; Fuentes-Aceituno, J.C.; Salinas-Rodríguez, A. The role of alkalizing agent on the manganese phosphating of a high strength steel part 1: The individual effect of NaOH and NH_4OH. *Surf. Coat. Technol.* **2016**, *291*, 179–188. [CrossRef]
9. Banczek, E.P.; Rodrigues, P.R.P.; Costa, I. The effects of niobium and nickel on the corrosion resistance of the zinc phosphate layers. *Surf. Coat. Technol.* **2008**, *202*, 2008–2014. [CrossRef]

10. Díaz, B.; Freire, L.; Mojío, M.; Nóvoa, X.R. Optimization of conversion coatings based on zinc phosphate on high strength steels, with enhanced barrier properties. *J. Electroanalyt. Chem.* **2015**, *737*, 174–183. [CrossRef]
11. Galvan-Reyes, C.; Salinas-Rodríguez, A.; Fuentes-Aceituno, J.C. Degradation and crystalline reorganization of hureaulite crystals during the manganese phosphating of a high strength steel. *Surf. Coat. Technol.* **2015**, *275*, 10–20. [CrossRef]
12. Weng, D.; Jokiel, P.; Uebleis, A.; Boehni, H. Corrosion and protection characteristics of zinc and manganese phosphate coatings. *Surf. Coat. Technol.* **1997**, *88*, 147–156. [CrossRef]
13. Narayanan, T.S. Influence of various factors on phosphatability—An overview. *Metal Finish.* **1996**, *94*, 86–90. [CrossRef]
14. Restifo, C.M.; Bainter, J.C. A new alternative to traditional iron phosphating for ferrous substrates. *Metal Finish.* **2000**, *98*, 44–47. [CrossRef]
15. Amini, R.; Vakili, H.; Ramezanzadeh, B. Studying the effects of poly (vinyl) alcohol on the morphology and anti-corrosion performance of phosphate coating applied on steel surface. *J. Taiwan Inst. Chem. Eng.* **2016**, *58*, 542–551. [CrossRef]
16. Ghali, E.L.; Potvin, R.J.A. The mechanism of phosphating of steel. *Corros. Sci.* **1972**, *12*, 583–594. [CrossRef]
17. Geometrical Product Specifications (GPS) Surface texture: Profile method-Terms, definitions and surface texture parameters. Available online: http://www.iso.org/iso/catalogue_detail.htm?csnumber=10132 (accessed on 11 October 2016).
18. Sadeghimeresht, E.; Markocsan, N.; Nylén, P. A Comparative Study of Corrosion Resistance for HVAF-Sprayed Fe- and Co-Based Coatings. *Coatings* **2016**, *6*, 16. [CrossRef]
19. Taghavikish, M.; Subianto, S.; Dutta, N.K.; Choudhury, N.R. Novel Thiol-Ene Hybrid Coating for Metal Protection. *Coatings* **2016**, *6*, 17. [CrossRef]
20. Pastorek, F.; Hadzima, B.; Doležal, P. Electrochemical characteristics of Mg-3Al-1Zn alloy surface with hydroxyapatite coating. *Communications* **2012**, *14*, 26–30.
21. Malshe, V.C.; Sikchi, M. *Basics of Paint Technology Part 2*; Antar Prakash Centre for Yoga: Hardwar, (Uttarakhand), India, 2008.
22. Hadzima, B.; Mhaede, M.; Pastorek, F. Electrochemical characteristics of calcium-phosphatized AZ31 Magnesium alloy in 0.9% NaCl Solution. *J. Mat. Sci. Mat. Med.* **2014**, *25*, 1227–1237. [CrossRef] [PubMed]
23. Jiang, X.P.; Wang, X.Y.; Li, J.X.; Li, D.Y.; Man, C.-S.; Shepard, M.J.; Zhai, T. Enhancement of fatigue and corrosion properties of pure Ti by sandblasting. *Mater. Sci. Eng. A* **2006**, *429*, 30–35. [CrossRef]
24. Wei, B.; Tokash, J.C.; Zhang, F.; Kim, Y.; Logan, B.E. Electrochemical analysis of separators used in single-chamber, air–cathode microbial fuel cells. *Electrochim. Acta* **2013**, *89*, 45–51. [CrossRef]
25. Han, X.G.; Zhu, F.; Zhu, X.P.; Lei, M.K.; Xu, J.J. Electrochemical corrosion behavior of modified MAO film on magnesium alloy AZ31 irradiated by high-intensity pulsed ion beam. *Surf. Coat. Technol.* **2013**, *228*, 164–170. [CrossRef]
26. Mhaede, M.; Pastorek, F.; Hadzima, B. Influence of shot peening on corrosion properties of biocompatible magnesium alloy AZ31 coated by dicalcium phosphate dihidrate (DCPD). *Mater. Sci. Eng.* **2014**, *39*, 330–335. [CrossRef] [PubMed]
27. Frankel, G.S. Electrochemical techniques in corrosion: Status, limitations, and needs. *J. ASTM Int.* **2008**, *5*, 3–40. [CrossRef]
28. Ariza, E.; Rocha, L.A. Evaluation of corrosion resistance of multi-layered Ti/glass–ceramic interfaces by electrochemical impedance spectroscopy. *Mater. Sci. Forum.* **2005**, *492*, 189–194. [CrossRef]
29. Skublova, L.; Hadzima, B.; Borbas, L.; Vitosova, M. The influence of temperature on corrosion properties of titanium and stainless steel biomaterials. *Mater. Eng.* **2008**, *15*, 18–22.